

## MAJOR PAPER

# Diagnostic Performance of Arterial Spin Labeling for Grading Nonenhancing Astrocytic Tumors

Delgerdalai Khashbat<sup>1</sup>, Masafumi Harada<sup>1</sup>, Takashi Abe<sup>1</sup>, Mungunbagana Ganbold<sup>1</sup>,  
Seiji Iwamoto<sup>1</sup>, Naoto Uyama<sup>1</sup>, Saho Irahara<sup>1</sup>, Youichi Otomi<sup>1</sup>,  
Teruyoshi Kageji<sup>2</sup>, and Shinji Nagahiro<sup>2</sup>

**Purpose:** We evaluated the utility of arterial spin labeling (ASL) imaging of tumor blood flow (TBF) for grading non-enhancing astrocytic tumors.

**Materials and Methods:** Thirteen non-enhancing astrocytomas were divided into high-grade ( $n = 7$ ) and low-grade ( $n = 6$ ) groups. Both ASL and conventional sequences were acquired using the same magnetic resonance machine. Intratumoral absolute maximum TBF ( $TBF_{max}$ ), absolute mean TBF ( $TBF_{mean}$ ), and corresponding values normalized to cerebral blood flow ( $TBF_{max}$  and  $TBF_{mean}$  ratios) were measured. The Mann-Whitney U test and receiver operating characteristic (ROC) curve analysis were used to assess the accuracy of TBF variables for tumor grading.

**Results:** Compared with low-grade astrocytoma, high-grade astrocytoma exhibited significantly greater absolute  $TBF_{max}$  ( $90.93 \pm 24.96$  vs  $46.94 \pm 20.97$  ml/100 g/min,  $P < 0.001$ ),  $TBF_{mean}$  ( $58.75 \pm 19.89$  vs  $31.16 \pm 17.63$  ml/100 g/min,  $P < 0.001$ ),  $TBF_{max}$  ratio ( $3.34 \pm 1.22$  vs  $1.35 \pm 0.5$ ,  $P < 0.001$ ), and  $TBF_{mean}$  ratio ( $2.15 \pm 0.94$  vs  $0.88 \pm 0.41$ ,  $P < 0.001$ ). The  $TBF_{max}$  ratio yielded the highest diagnostic accuracy (sensitivity 100%, specificity 86.3%), while absolute  $TBF_{mean}$  yielded the lowest accuracy (sensitivity 85.7%, specificity 70.1%) by ROC analysis.

**Conclusion:** Parameters from ASL perfusion imaging, particularly  $TBF_{max}$  ratio, may be useful for distinguishing high-grade from low-grade astrocytoma in cases with equivocal conventional MRI findings.

**Keywords:** arterial spin labeling, astrocytoma grading, nonenhancing, perfusion

## Introduction

Astrocytic tumor is the most common primary brain tumor in adults. The grading of astrocytic tumors is important for prognosis and for choosing the optimal treatment strategy.<sup>1,2</sup> In general, high-grade astrocytomas (HGAs) exhibit signal enhancement on post-contrast MRI due to blood-brain barrier disruption with neovascularization, while low-grade astrocytomas (LGAs) are homogeneously nonenhancing.<sup>3,4</sup> However, some malignant astrocytomas can also be nonenhancing

on traditional MRI modalities, leading to misdiagnosis of tumor grade.<sup>5–7</sup>

When traditional MRI methods are insufficient for tumor characterization, advanced imaging methods such as gadolinium-based perfusion-weighted MRI can predict histopathologic grade by revealing signs of microvessel proliferation.<sup>3,7–10</sup> Cerebral perfusion can also be measured using non-contrast arterial spin labeling (ASL) perfusion imaging, which estimates cerebral tissue blood flow using magnetically labeled arterial blood water as an endogenous tracer.<sup>11</sup> The absence of an exogenous contrast agent may make ASL preferable as a reproducible, quantitative technique in daily clinical practice.<sup>12,13</sup> Indeed, multiple studies have reported strong correlations between ASL and gadolinium-based dynamic susceptibility contrast (DSC) MRI in brain tumor diagnosis and grading.<sup>14–16</sup> In addition, several studies have demonstrated that tumor blood flow (TBF) estimated by preoperative ASL can discriminate low- from high-grade astroglial tumors.<sup>14,17–19</sup> However, ASL has not yet been characterized for the evaluation of nonenhancing brain tumors. In this study, we assessed

<sup>1</sup>Departments of Radiology and Radiation Oncology, Institute of Biomedical Sciences, Tokushima University Graduate School, 3-18-15 Kuramoto-cho, Tokushima, Tokushima 770-8509, Japan

<sup>2</sup>Department of Neurosurgery, Institute of Biomedical Sciences, Tokushima University Graduate School, Tokushima, Japan

\*Corresponding author, Phone: +81-88-633-9283, Fax: +81-88-633-7174, E-mail: delgerdalaikh@gmail.com

©2017 Japanese Society for Magnetic Resonance in Medicine  
This work is licensed under a Creative Commons Attribution-NonCommercial-NoDerivatives International License.

Received: April 30, 2017 | Accepted: October 25, 2017

the diagnostic utility of ASL for grading nonenhancing astrocytic tumors.

## Materials and Methods

### Patients

This retrospective study was approved by the Tokushima University ethics committee and written informed consent was obtained from all patients prior to enrollment. We reviewed our institutional database between 2010 and 2016, and included only patients meeting the following criteria: 1) histopathologically confirmed astrocytoma, 2) no contrast enhancement on post-contrast T<sub>1</sub>-weighted imaging (CE + T<sub>1</sub>WI), 3) no treatment history before MRI examination, and 4) conventional and ASL parameters obtained on the same MR machine. We did not include pilocytic astrocytoma, which frequently occurs in pediatric patients.<sup>20</sup>

Finally, 13 patients with nonenhancing astrocytoma (seven men and six women; age 52.15 ± 17.98 years; range, 19–77 years) were included and divided into high-grade ( $n = 7$ ) and low-grade ( $n = 6$ ) groups based on the 2007 World Health Organization (WHO) classification.<sup>1</sup> Total resection was performed in six cases (five HGAs, one LGA), partial resection in three cases (one HGA, two LGAs), and a biopsy in four cases (one HGA, three LGAs).

### MRI protocols

All MR images (CE + T<sub>1</sub>WI, T<sub>2</sub>WI, fluid attenuated inversion recovery [FLAIR], T<sub>1</sub>WI, DWI, and ASL) were acquired on the same 3T scanner (Discovery 750 3.0T; GE Healthcare, Milwaukee, WI, USA) using a standard 8-channel head coil.

CE + T<sub>1</sub>-weighted images were acquired using a 3D fast spoiled gradient-echo (FSPGR) sequence after injection of 0.1 mmol/kg body weight gadopentetate dimeglumine Gd-DTPA (Magnevist; Bayer HealthCare, Berlin, Germany) using a power injector (Medrad Inc, Indianola, PA, USA) at 2.5 ml/s followed by a normal saline (20 ml) lock-flush at the same rate. Scan parameters for 3D FSPGR were TR 10.4 ms, TE 4.4 ms, bandwidth 31.25 kHz, slice thickness 1.2 mm, matrix 384 × 256, flip angle (FA) 15°, number of excitations (NEX) 1, FOV 24 × 24 cm, acceleration factor 2 × 2, number of slices 160, and acquisition time of 3:34 min.

Axial T<sub>2</sub>-weighted images were acquired using a fast recovery fast spin-echo (FRFSE) sequence with the following parameters: TR 3000 ms, TE 96 ms, bandwidth 125.00 kHz, slice thickness 5 mm, matrix 256 × 256, echo train length 12, FA 111°, NEX 1, FOV 24 × 24 cm, acceleration factor 2 × 2, number of slices 25, and acquisition time of 3:34 min.

The ASL images were acquired as described previously.<sup>21</sup> Briefly, ASL was performed with pseudo-continuous labeling, background suppression, and a stack of spiral 3D fast spin-echo imaging sequences using the following acquisition parameters: 512 sampling points on eight spirals, FOV

24 cm, TR 4632 ms, TE 10.5 ms, reconstructed matrix size 64 × 64, number of excitation 2, labeling duration 1650 ms, post-labeling delay 1525 ms, slice thickness 4 mm, number of slices 36, and acquisition time of 3:15 min.

### Data analysis

ASL and conventional MRI data were transferred to a workstation with commercially available software (Advantage workstation AW 4.6; GE Healthcare). Two neuroradiologists (K.D and H.M., with 7 and 20 years of experience, respectively) assessed the MR images, and confirmed that none of these tumors was presented any contrast enhancement on CE + T<sub>1</sub>WI. The placement of ROIs was also defined by the two neuroradiologists who were not provided knowledge of histopathological information.

Next, all measurements were performed by a neuroradiologist (K.D) who has neuroimaging research experience. For each tumor, five circular ROIs (approximately 150 mm<sup>2</sup> each) were manually drawn on the middle of the tumor by using two to three trans-axial slices had the largest tumoral hyperintensity for T<sub>2</sub>WI while avoiding areas of large vascular, non-tumoral, calcified, or hemorrhagic. All ROIs were copied to the corresponding ASL map.

Other conventional MR sequences such as CE + T<sub>1</sub>WI, FLAIR, and T<sub>1</sub>WI were also used as references for defining tumor position.

We measured absolute maximum TBF (TBF<sub>max</sub>) and absolute mean TBF (TBF<sub>mean</sub>) of the five ROIs, and the corresponding TBF values normalized by cerebellum (TBF<sub>max</sub> ratio and TBF<sub>mean</sub> ratio, respectively). For the relative TBF measurements in each patient, a total of four circular ROIs (approximately 200 mm<sup>3</sup>) were performed in the bilateral cerebellar hemispheres, including both white and gray matter areas; then, the averaged mean cerebral blood flow (CBF) values from these reference ROIs were used for further analysis. Use a cerebellar reference region for normalization was described previously.<sup>16</sup>

### Statistical analysis

All statistical analysis was performed using SPSS Ver. 20 (IBM, Armonk, NY, USA). The Mann-Whitney U test was used to compare ASL TBF measurements between LGA and HGA. Receiver operating characteristic (ROC) curve analysis was used to assess the diagnostic accuracy of these TBF parameters for differentiating tumor grades. Data are presented as means ± standard deviation (SD). All statistical tests were two-tailed and a  $P < 0.05$  was considered significant.

## Results

In this study, 7 of the 13 nonenhancing astrocytic tumors (53.8%) were high-grade according to WHO criteria. There was no significant difference in mean age or sex ratio between HGA and LGA groups. Individual tumor characteristics and the ROI values of all TBF variables are presented in Table 1.

**Table 1** Patient and tumor characteristics

| Tumor (No.)        | Age (years) | Sex | Histopathological diagnosis | WHO grade | TBF <sub>max</sub> (ml/100 g/min) | TBF <sub>mean</sub> (ml/100 g/min) | TBF <sub>max</sub> ratio | TBF <sub>mean</sub> ratio |
|--------------------|-------------|-----|-----------------------------|-----------|-----------------------------------|------------------------------------|--------------------------|---------------------------|
| Low-grade (n = 6)  |             |     |                             |           |                                   |                                    |                          |                           |
| 1                  | 65          | m   | DA                          | II        | 42.24                             | 31.12                              | 1.07                     | 0.79                      |
| 2                  | 40          | f   | DA                          | II        | 28.41                             | 17.4                               | 0.88                     | 0.54                      |
| 3                  | 67          | f   | DA                          | II        | 84.86                             | 61.72                              | 2.11                     | 1.56                      |
| 4                  | 54          | f   | DA                          | II        | 33.14                             | 17.87                              | 1.73                     | 0.93                      |
| 5                  | 40          | m   | DA                          | II        | 58.10                             | 38.49                              | 1.41                     | 0.92                      |
| 6                  | 31          | f   | DA                          | II        | 28.43                             | 20.36                              | 0.94                     | 0.55                      |
| High-grade (n = 7) |             |     |                             |           |                                   |                                    |                          |                           |
| 7                  | 69          | f   | AA                          | III       | 83.76                             | 64.56                              | 2.7                      | 2.08                      |
| 8                  | 34          | m   | AA                          | III       | 70.20                             | 36.28                              | 2.28                     | 1.18                      |
| 9                  | 19          | f   | AA                          | III       | 58.32                             | 34.00                              | 2.12                     | 1.14                      |
| 10                 | 53          | m   | AA                          | III       | 100.67                            | 54.43                              | 3.94                     | 2.13                      |
| 11                 | 72          | m   | GBM                         | IV        | 117.19                            | 83.11                              | 5.53                     | 3.92                      |
| 12                 | 77          | m   | GC                          | IV        | 92.61                             | 66.48                              | 3.50                     | 2.51                      |
| 13                 | 57          | m   | GBM                         | IV        | 113.78                            | 72.23                              | 3.37                     | 2.14                      |

Perfusion data are shown by the average values of five ROIs for each patient. AA, anaplastic astrocytoma; DA, diffuse astrocytoma; GBM, glioblastoma multiforme; GC, gliomatosis cerebri; max, maximum; TBF, tumor blood flow; WHO, World Health Organization.

Absolute and normalized TBF<sub>max</sub> values were significantly higher in HGA than in LGA (absolute TBF<sub>max</sub>: 90.93 ± 24.96 vs 46.94 ± 20.97 ml/100 g/min,  $P < 0.001$ ; absolute TBF<sub>mean</sub>: 58.75 ± 19.89 vs 31.16 ± 17.63 ml/100 g/min,  $P < 0.001$ ; TBF<sub>max</sub> ratio: 3.34 ± 1.22 vs 1.35 ± 0.5,  $P < 0.001$ ; TBF<sub>mean</sub> ratio: 2.15 ± 0.94 vs 0.88 ± 0.41,  $P < 0.001$ ). The diagnostic accuracy of all ASL parameters for distinguishing HGA from LGA was examined by ROC analysis (Fig. 1). The area under curve (AUC) was 0.910 for TBF<sub>max</sub>, 0.852 for TBF<sub>mean</sub>, 0.974 for TBF<sub>max</sub> ratio, and 0.917 for TBF<sub>mean</sub> ratio. Absolute TBF<sub>max</sub> with a cut-off value of 62.91 ml/100 g/min discriminated HGA from LGA with 91.4% sensitivity and 83.3% specificity, while TBF<sub>max</sub> ratio with a cut-off of 1.90 discriminated HGA from LGA with 100% sensitivity and 86.3% specificity. Mean TBF values were less accurate; absolute TBF<sub>mean</sub> with a cut-off of 40.37 ml/100 g/min yielded 85.7% sensitivity and 70.1% specificity, while TBF<sub>mean</sub> ratio with a cut-off of 1.18 distinguished HGA from LGA with 91.4% sensitivity and 76.3% specificity. Representative images from cases with HGA and LGA are illustrated in Figs. 2 and 3.

## Discussion

Characterization of nonenhancing malignant astrocytoma has always been a challenge using conventional MRI. Furthermore, the relationship between tumor histopathologic grade and degree of contrast enhancement is not definitive. About 40% of nonenhancing brain neoplasm could be malignant,<sup>7,8</sup> whereas some LGAs show contrast intensity.<sup>22</sup>

The optimal treatment strategy differs according to grade. Maximum surgical resection of tumor tissue is necessary for HGA, while radiotherapy and monitoring are often recommended for LGAs. Even with optimal treatment, survival time is only 1.5–5 years for HGA compared to 8–10 years or more for LGA.<sup>2,4,23</sup> Earlier and more accurate differentiation may improve these survival rates.

Histopathologic HGA is highly vascular, while angiogenesis in LGA resembles that of normal brain. ASL perfusion imaging can define tumor grade and type according to microvessel density.<sup>15,17</sup> Indeed, all TBF parameters measured in this study were greater in HGA. However, absolute TBF<sub>max</sub> and TBF<sub>max</sub> ratio were more accurate than either TBF<sub>mean</sub> parameter (Fig. 1). Most previous studies of ASL for glioma grading,<sup>12,14</sup> including astrocytomas,<sup>19</sup> also found that absolute TBF<sub>max</sub> and TBF<sub>max</sub> ratio were most accurate, with sensitivity up to 100%. It is known that ASL is sensitive to arterial transit time, which in turn varies markedly among healthy individuals depending on age, sex, and other factors.<sup>14,24</sup> Tumor neovascularity is heterogeneously abnormal (including tortuous, expanded, and permeable regions), which creates substantial variation in transit time.<sup>25</sup> Presumably, normalization controls for a fraction of this individual variability among subjects and thus yields improved grading accuracy.

In this study, none of the HGAs had perfusion values below the cut-off (Table 1) and only one LGA showed perfusion above the cut-off, a finding consistent with a rCBV map derived from DSC MRI (data not shown). The two cases of grade IV astrocytoma (glioblastoma multiforme [GBM])

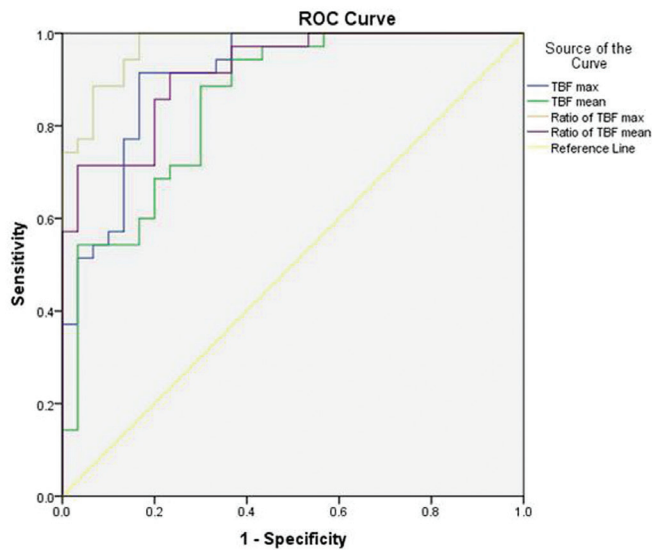


**Fig. 1** Receiver operating characteristic (ROC) curves of arterial spin labeling (ASL)-derived tumor blood flow (TBF) variables for the grading of nonenhancing astrocytoma.

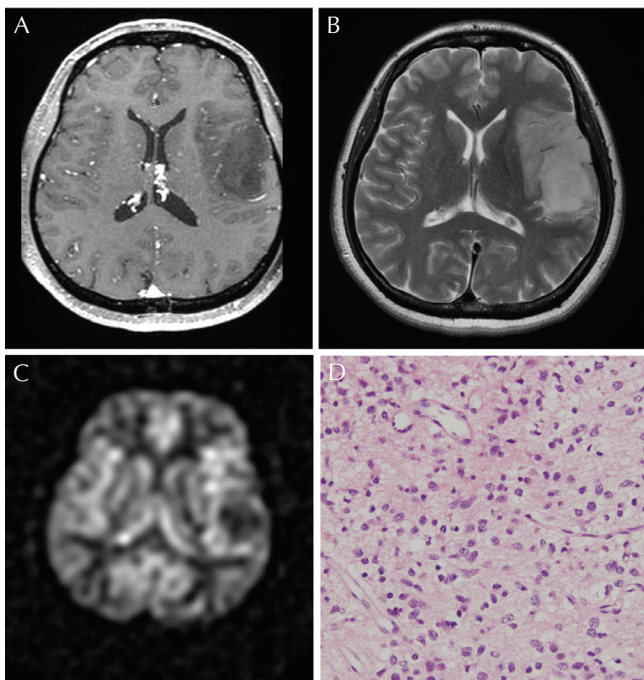


**Fig. 2** A 40-year-old female patient with low-grade astrocytoma (World Health Organization [WHO] grade II, diffuse astrocytoma). (A and B) Tumor shows no contrast enhancement on contrast enhancement on post-contrast  $T_1$ -weighted imaging (CE +  $T_1$ WI) (A) but hyperintensity on  $T_2$ WI (B). (C) Tumor shows hypoperfusion on the arterial spin labeling (ASL) perfusion map. (D) Hematoxylin and eosin,  $\times 100/200$ , there is a modest increase in cellularity and nuclear atypia.

included in this series demonstrated the greatest perfusion values (Table 1). The appearance of nonenhancing GBM on ASL perfusion imaging is similar to that of typical GBM, showing markedly hyper-perfusion. Multiple studies have

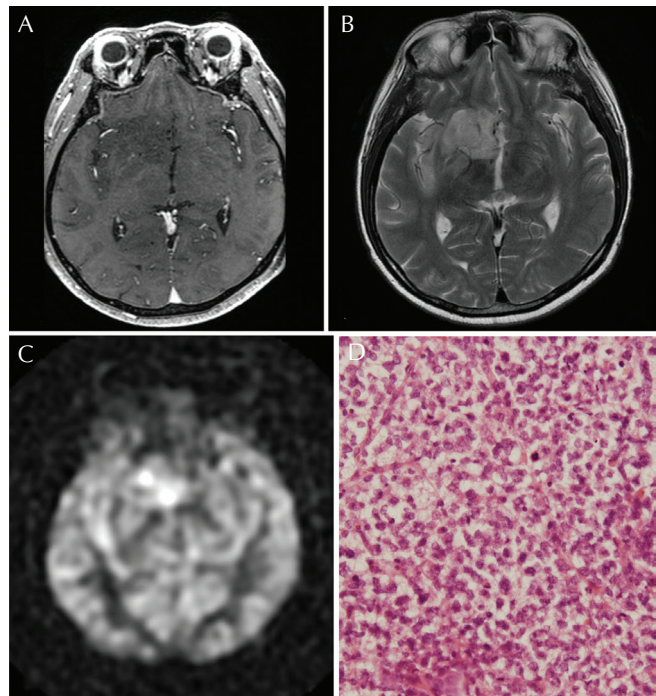


**Fig. 3** A 57-year-old male patient with nonenhancing high-grade astrocytoma histopathologically confirmed as World Health Organization (WHO) grade IV (glioblastoma multiforme [GBM]). (A) Tumor shows no contrast enhancement and hypointensity on contrast enhancement on post-contrast  $T_1$ -weighted imaging (CE +  $T_1$ WI). (B) On  $T_2$ WI, tumor exhibits hyperintensity. (C) ASL perfusion map demonstrates marked hyperperfusion of the tumor lesion. (D) Hematoxylin and eosin,  $\times 100/200$ , monomorphic cells congregate in high density. Mitoses and apoptosis are frequent.

reported initially nonenhancing GBM with emergence of contrast on MRI over ensuing months.<sup>6,26,27</sup> Thus, ASL may allow for earlier detection of initially nonenhancing GBM. Further, early detection of LGA may prolong survival given that about 40% eventually undergo malignant transformation.<sup>1,2,6,22,23</sup>

Contrast-based DSC MRI is currently the primary modality for cerebral perfusion measurements. Relative tumor blood volume (rTBV) measurement by DSC MRI positively correlated with nonenhancing glioma grade and discriminated low-grade diffuse astrocytoma from other low-grade gliomas or anaplastic tumors.<sup>3,7-9</sup> Morita et al.<sup>7</sup> graded nonenhancing pure astrocytomas with sensitivity of 90.9% and specificity of 100% using a rTBF cut-off value of 1.94. Similarly, a CT perfusion study distinguishing nonenhancing gliomas as grade II or III achieved 83.3% sensitivity and 90.9% specificity using rTBV and 83.3% sensitivity and 81.8% specificity using rTBF.<sup>28</sup> Thus, relative tumor perfusion parameters derived from multiple modalities, including ASL, can successfully grade nonenhancing astrocytomas.

Alternatively, several studies using DSC MRI found no significant difference in rTBV among histopathological grades of nonenhancing glial tumors, including both oligodendrogliomas and astrocytomas.<sup>29,30</sup> It is known that

oligodendroglial tumors contain dense vascular networks, and thus could exhibit high perfusion.<sup>31</sup> Low-grade oligodendrogliomas often exhibit higher perfusion than LGAs.<sup>3</sup> Sometimes, it can also be indistinguishable from high-grade oligodendroglioma on contrast perfusion modality.<sup>32</sup> A previous study reported that using ASL with low-grade oligodendrogliomas showed elevated perfusion values while high-grade oligodendroglial tumors exhibited decreased perfusion measurements.<sup>33</sup> Probably, the inclusion of oligodendrogliomas would also affect the reliability of ASL imaging for nonenhancing grading gliomas.

In addition to these perfusion imaging modalities, MR spectroscopy, diffusion MRI, and positron emission tomography (PET) are also used for the assessment of nonenhancing brain tumors.<sup>29,30,34</sup> However, no study examined the utility of ASL imaging for nonenhancing brain tumor grading. We suggest that ASL is another useful modality for preoperative grading of nonenhancing astrocytic tumors.

In the clinical setting, the role of ASL for brain tumor assessment has progressively expanded due to advantages such as repeatability in the absence of contrast agents such as gadolinium (Gd). Thus, ASL may prove to be a better option for brain tumor grading and treatment response in patients with renal insufficiency. Further, recent improvements in ASL perfusion imaging have resulted in higher signal-to-noise ratio, fewer artifacts, and 3D imaging with background suppression.<sup>12</sup> However, the transit delay effect remains an outstanding limitation to the accuracy of ASL, especially for cerebrovascular-occlusive diseases with long transit time. For compensation of transit time effect, post-labeling delay is applied in most ASL applications.<sup>13</sup>

Limitations of this study include the small number of patients. However, most previous studies of nonenhancing brain tumors also included a small number of cases due to the rarity of nonenhancing malignant astrocytoma. Moreover, histopathologic examination of resection or biopsy samples is not always immediately performed for low-grade tumors,<sup>4,22,23</sup> which may have limited the inclusion of some nonenhancing brain tumors that were clinically suggestive of astrocytoma. We did not include gliomas with oligodendroglial components in the present analysis, but there is no standard criteria in differentiating astrocytomas from oligodendrogliomas. Therefore, gliomas can occur mixed form in containing both of oligodendroglial and astrocytic tumor cells that is a common subtype of glial tumors.<sup>1</sup> On the other hand, oligodendroglial tumors are more chemosensitive and have better prognosis than astrocytic tumors.<sup>2,7,23</sup>

The histopathological diagnosis of some tumors in the current series was confirmed by either biopsy or partial resection. However, biopsy and partial resection are less invasive and have a lower mortality rate compared to total resection; the sampling error for a biopsy or small amount of tumor resection cannot assess the total tumor area, which can sometimes lead to insufficient determination of tumor grade. Alternatively, advanced MRI techniques such as spectroscopy,

permeability, and perfusion were performed for all the tumor cases, aiding in more accurate tumor grading. Despite these limitations, the diagnostic utility of ASL for astrocytoma grading warrants larger-scale studies given the high accuracy observed in this small sample.

In summary, ASL perfusion imaging successfully distinguished LGA and HGA and therefore could be useful for preoperative grading of nonenhancing brain tumors. Among perfusion parameters evaluated, normalized maximal TBF provided the highest diagnostic accuracy for the tumor grade.

## Acknowledgement

This work is partly supported by KAKENHI, a Grant-in-Aid for Scientific Research (C) 15K09926 from Japanese Society for the Promotion of Science.

## Conflicts of Interest

The authors declare that they have no conflicts of interest.

## References

1. Louis DN, Ohgaki H, Wiestler OD, et al. The 2007 WHO classification of tumours of the central nervous system. *Acta Neuropathol* 2007; 114:97–109.
2. Stupp R, Brada M, van den Bent MJ, Tonn JC, Pentheroudakis G, Group EGW. High-grade glioma: ESMO Clinical Practice Guidelines for diagnosis, treatment and follow-up. *Ann Oncol* 2014; 25 Suppl 3:iii93–iii101.
3. Maia AC, Malheiros SM, da Rocha AJ, et al. Stereotactic biopsy guidance in adults with supratentorial nonenhancing gliomas: role of perfusion-weighted magnetic resonance imaging. *J Neurosurg* 2004; 101:970–976.
4. Pedersen CL, Romner B. Current treatment of low grade astrocytoma: a review. *Clin Neurol Neurosurg* 2013; 115:1–8.
5. Ginsberg LE, Fuller GN, Hashmi M, Leeds NE, Schomer DF. The significance of lack of MR contrast enhancement of supratentorial brain tumors in adults: histopathological evaluation of a series. *Surg Neurol* 1998; 49: 436–440.
6. Cohen-Gadol AA, DiLuna ML, Bannykh SI, Piepmeier JM, Spencer DD. Non-enhancing de novo glioblastoma: report of two cases. *Neurosurg Rev* 2004; 27:281–285.
7. Morita N, Wang S, Chawla S, Poptani H, Melhem ER. Dynamic susceptibility contrast perfusion weighted imaging in grading of nonenhancing astrocytomas. *J Magn Reson Imaging* 2010; 32:803–808.
8. Batra A, Tripathi RP, Singh AK. Perfusion magnetic resonance imaging and magnetic resonance spectroscopy of cerebral gliomas showing imperceptible contrast enhancement on conventional magnetic resonance imaging. *Australas Radiol* 2004; 48:324–332.
9. Fan GG, Deng QL, Wu ZH, Guo QY. Usefulness of diffusion/perfusion-weighted MRI in patients with non-enhancing supratentorial brain gliomas: a valuable tool to predict tumour grading? *Br J Radiol* 2006; 79:652–658.

10. Server A, Graff BA, Orheim TE, et al. Measurements of diagnostic examination performance and correlation analysis using microvascular leakage, cerebral blood volume, and blood flow derived from 3T dynamic susceptibility-weighted contrast-enhanced perfusion MR imaging in glial tumor grading. *Neuroradiology* 2011; 53:435–447.
11. Detre JA, Alsop DC. Perfusion magnetic resonance imaging with continuous arterial spin labeling: methods and clinical applications in the central nervous system. *Eur J Radiol* 1999; 30:115–124.
12. Wolf RL, Detre JA. Clinical neuroimaging using arterial spin-labeled perfusion magnetic resonance imaging. *Neurotherapeutics* 2007; 4:346–359.
13. Detre JA, Rao H, Wang DJ, Chen YF, Wang Z. Applications of arterial spin labeled MRI in the brain. *J Magn Reson Imaging* 2012; 35:1026–1037.
14. Warmuth C, Gunther M, Zimmer C. Quantification of blood flow in brain tumors: comparison of arterial spin labeling and dynamic susceptibility-weighted contrast-enhanced MR imaging. *Radiology* 2003; 228:523–532.
15. Kimura H, Takeuchi H, Koshimoto Y, et al. Perfusion imaging of meningioma by using continuous arterial spin-labeling: comparison with dynamic susceptibility-weighted contrast-enhanced MR images and histopathologic features. *AJNR Am J Neuroradiol* 2006; 27:85–93.
16. Järnum H, Steffensen EG, Knutsson L, et al. Perfusion MRI of brain tumours: a comparative study of pseudo-continuous arterial spin labelling and dynamic susceptibility contrast imaging. *Neuroradiology* 2010; 52:307–317.
17. Noguchi T, Yoshiura T, Hiwatashi A, et al. Perfusion imaging of brain tumors using arterial spin-labeling: correlation with histopathologic vascular density. *AJNR Am J Neuroradiol* 2008; 29:688–693.
18. Hirai T, Kitajima M, Nakamura H, et al. Quantitative blood flow measurements in gliomas using arterial spin-labeling at 3T: intermodality agreement and inter- and intraobserver reproducibility study. *AJNR Am J Neuroradiol* 2011; 32:2073–2079.
19. Xiao HF, Chen ZY, Lou X, et al. Astrocytic tumour grading: a comparative study of three-dimensional pseudocontinuous arterial spin labelling, dynamic susceptibility contrast-enhanced perfusion-weighted imaging, and diffusion-weighted imaging. *Eur Radiol* 2015; 25:3423–3430.
20. Koeller KK, Rushing EJ. From the archives of the AFIP: pilocytic astrocytoma: radiologic-pathologic correlation. *Radiographics* 2004; 24:1693–1708.
21. Dai W, Garcia D, de Bazelaire C, Alsop DC. Continuous flow-driven inversion for arterial spin labeling using pulsed radio frequency and gradient fields. *Magn Reson Med* 2008; 60:1488–1497.
22. Pallud J, Capelle L, Taillandier L, et al. Prognostic significance of imaging contrast enhancement for WHO grade II gliomas. *Neuro-oncology* 2009; 11:176–182.
23. Youland RS, Schomas DA, Brown PD, et al. Changes in presentation, treatment, and outcomes of adult low-grade gliomas over the past fifty years. *Neuro-oncology* 2013; 15:1102–1110.
24. Liu Y, Zhu X, Feinberg D, et al. Arterial spin labeling MRI study of age and gender effects on brain perfusion hemodynamics. *Magn Reson Med* 2012; 68:912–922.
25. Silva AC, Kim SG, Garwood M. Imaging blood flow in brain tumors using arterial spin labeling. *Magn Reson Med* 2000; 44:169–173.
26. Utsuki S, Oka H, Miyajima Y, Kijima C, Yasui Y, Fujii K. Glioblastoma without remarkable contrast enhancement on magnetic resonance imaging. *Int J Clin Med* 2012; 3:439–445.
27. Ideguchi M, Kajiwara K, Goto H, et al. MRI findings and pathological features in early-stage glioblastoma. *J Neurooncol* 2015; 123:289–297.
28. Beppu T, Sasaki M, Kudo K, et al. Prediction of malignancy grading using computed tomography perfusion imaging in nonenhancing supratentorial gliomas. *J Neurooncol* 2011; 103:619–627.
29. Liu X, Tian W, Kolar B, et al. MR diffusion tensor and perfusion-weighted imaging in preoperative grading of supratentorial nonenhancing gliomas. *Neuro-oncology* 2011; 13:447–455.
30. Sahin N, Melhem ER, Wang S, et al. Advanced MR imaging techniques in the evaluation of nonenhancing gliomas: perfusion-weighted imaging compared with proton magnetic resonance spectroscopy and tumor grade. *Neuroradiol J* 2013; 26:531–541.
31. Cha S. Update on brain tumor imaging: from anatomy to physiology. *AJNR Am J Neuroradiol* 2006; 27:475–487.
32. Xu M, See SJ, Ng WH, et al. Comparison of magnetic resonance spectroscopy and perfusion-weighted imaging in presurgical grading of oligodendroglial tumors. *Neurosurgery* 2005; 56:919–926.
33. Wolf RL, Wang J, Wang S, et al. Grading of CNS neoplasms using continuous arterial spin labeled perfusion MR imaging at 3 Tesla. *J Magn Reson Imaging* 2005; 22:475–482.
34. Watanabe A, Muragaki Y, Maruyama T, Shinoda J, Okada Y. Usefulness of <sup>11</sup>C-methionine positron emission tomography for treatment-decision making in cases of non-enhancing glioma-like brain lesions. *J Neurooncol* 2016; 126:577–583.